UNIVERSIDAD DE LAS PALMAS DE GRAN CANARIA

DEPARTAMENTO DE BIOLOGÍA

OCEANOGRAFÍA BIOLÓGICA

PHYTOPLANKTON COMMUNITY COMPOSITION AND SIZE-ABUNDANCE SPECTRA IN AREAS OF THE ALBORÁN SEA WITH DIFFERENT HYDROLOGICAL CHARACTERISTICS

Memoria de Investigación presentada por la Lcda. Dña. Iria Sala Martínez

Directores: Dra. Dña. Lidia Yebra Mora y Dr. D. Jesús M. Mercado Carmona.

Tutora: Dra. Dña. María Milagrosa Gómez Cabrera.

Las Palmas de Gran Canaria, a 4 de Febrero de 2011

A mis directores, Lidia y Jesús, por su ayuda, orientación y apoyo a lo largo de estos meses.

A mis compañeros de despacho que me han hecho sentir como en casa. En especial a Soluna, por todos esos conocimientos fitoplanctónicos que ha compartido conmigo.

A mis vecinas al otro lado del pasillo, en especial a Elvira, por estar siempre dispuestas a alegrame el día.

A mis amigos, en especial a Ángela y a Fer, por estar siempre ahí, contra viento y marea.

A mi madre y a mi hermana, por creer en mi más que yo misma, por ayudarme a no rendirme. Os quiero!

A mi padre.

Phytoplankton community composition and size-abundance spectra in areas of the Alborán Sea with different hydrological characteristics

Iria Sala*, Lidia Yebra, Jesús M. Mercado and Soluna Salles

Instituto Español de Oceanografía, Centro Oceanográfico de Málaga, Apdo. 285, 29640 Fuengirola, Málaga, Spain

Corresponding author: E-mail: iria.sala@ma.ieo.es

Tel. +34-952-460-205, fax +34-952-463-808

ABSTRACT

Size-abundance spectra (SAS) were analyzed in different phytoplankton assemblages of the Alborán Sea collected in areas with contrasting hydrological features (upwelling areas and anticyclonic gyre). Abundance of micro-plankton cells decreased following the hydrological gradient from the most productive stations towards offshore stations. This size-fraction of phytoplankton was dominated by diatoms. Pico-plankton followed an opposite gradient. Concordantly, the slope of the SAS trended to decrease from coastal areas (upwelling) towards the anticyclonic gyre. However, phytoplankton assemblages featuring similar SAS values presented a quite different taxonomical composition of their diatom communities. According to the previous available information about the taxonomical composition of the phytoplankton communities in the Alborán Sea, these differences in diatom composition are indicative of differences in productivity of the phytoplankton. Consequently, the utility of phytoplankton SAS as an indicator of changes in the phytoplankton communities of the Alborán Sea is discussed.

Key words: size-abundance spectra, phytoplankton composition, Alborán Sea.

INTRODUCTION

The size structure of the phytoplankton communities has been proposed by Legendre and Le Févre (1991) as a tool to determine whether the energy in the pelagic trophic web flows through a "microbial" or an "herbivore" pathway. It is normally considered that the phytoplankton community is constituted predominantly by small autotrophic organisms in stratified and oligotrophic waters where the microbial food web the predominant pathway to the energy flow (Azam et al., 1983). In contrast, in turbulent and richer areas, where the large phytoplankton cells are comparatively more abundant, the herbivore pathway is assumed to be predominant (Steele, 1974; Delgado, 1990). Numerous subsequent studies demonstrate that this paradigm is an over-simplification of the factual situation normally found in the ocean. Different studies indicate that changes in larger size fractions of phytoplankton are responsible for most of the variability in total phytoplankton biomass while the abundance of picophytoplankton is relatively constant (Raimbault et al., 1988; Rodríguez et al., 1998 among others). Consequently, the microbial food web is in a continuous functioning while the herbivorous food web is relevant when nutrients are injected into upper layers of the water column (Thingstad and Sakshaug, 1990; Arin et al., 2002). If large cells contribution is responsible of the enhancements in productivity, changes in total primary production should always be associated with modifications in size distribution and food-web structure.

The Alborán Sea is the westernmost basin in the Mediterranean Sea, being the first basin for inflow of Atlantic water trough the Gibraltar Strait. The superficial inflow of Atlantic water through the Strait of Gibraltar produces a system with two quasi-persistent anticyclonic gyres (Parrilla and Kinder, 1985; Minas et al., 1991; Tintoré et al., 1991), which occupy the entire central part of the Alborán Sea. Besides, the Atlantic water jet produces an intensive geostrophyc front in the north-western sector of the basin (Parrilla

and Kinder, 1987; Sarhan *et al*., 2000) that causes intermittent events of upwelling of deep Mediterranean water enriched in inorganic nutrients off the Málaga coast (one of the most productive areas in the western Mediterranean Sea), in contrast with the more oligotrophic waters found at the centre of anticyclonic gyre. The remarkable hydrodynamism found in the Alborán Sea offers a suitable scenario for the study of the effect of hydrological variability on the size structure of the phytoplankton assemblages (Arin et al., 2002; Ramírez et al., 2005; Mercado et al. 2005, 2006 and 2007; among others). In this study we compared the phytoplankton composition and the size-abundance spectra of the phytoplankton communities growing under contrasting hydrological conditions found in different areas of the Alborán Sea, in order to evaluate the contribution of different phytoplankton groups to the size structure of the communities and to assess the hypothesis that changes in size-structure are mainly due to larger cells.

MATERIAL AND METHODS

The data analysed in this work were collected in the North Alborán Sea (35º 54' – 36º 33' N and 4º 11' – 4º 54' W) during a oceanographic survey performed in the framework of Project Nitroalboran that was conducted between 9th and 14th of May 2008 on board R/V García del Cid. Ten stations distributed into two transects following a gradient from the coast to the open sea were analysed (Fig. 1). At each sampling station, a SeaBird25 CTD was deployed between 0 and 100 m to obtain vertical profiles of salinity, temperature and fluorescence. Water samples were obtained at superficial and maximum subsurface fluorescence (MSF) depths using 12 L Niskin bottles. The surface sampling depth was established at 5 m for all stations, while the MSF depth was determined after examining the fluorescence profiles.

Nutrients (NO_3 and PO_4) and chlorophyll *a* concentrations were analysed as described in

Ramiréz et al. (2005). Abundance of picoplankton and nanoplankton was determined by a Becton Dickinson FACScan flow cytometer (FC) from samples fixed with glutaraldehyde (1% f.c.) and frozen in liquid nitrogen (Vaulot et al., 1989). The biovolumes of *Synechococcus*, *Prochlorococcus*, nanoeukaryotes and picoeukaryotes were calculated using the values given in Ribes et al. (1999) for samples from the Northwestern Mediterranean Sea.

Additional water samples were fixed in dark glass bottles with Lugol's solution (2% f.c.) for analysis of abundance and taxonomy of microplankton. In the laboratory, 100 mL of the fixed sample were sedimented in a composite chamber for 48 h following the technique developed by Utermöhl (1958). Cells were counted at 200x and 400x with an inverted microscope Leica DMIL connected to a Leica DFC video-camera as described in Mercado et al. (2005). The taxonomic composition of the phytoplankton communities in each sample was determined from the image analysis (IA) performed with Leica Application Suite software. The species nomenclature was validated following Tomas (1997). Cell biovolumes were calculated from cell-size and shape by using the most appropriate geometric formulas (Table 1). In total, 1,040 cells of phytoplankton were measured. A mean value of biovolume was calculated for each species or group listed in Table 1. For some species (*Pleurosigma spp*., *Disposals spp*., *Oxitoxum spp*. and *Dyctiocha spp*.) only one cell could be measured. For the genus *Nitzschia* and *Ceratium* a mean biovolumen was calculated from the values obtained for the different species identified.

In order to elaborate the size-abundance spectra (SAS), the taxonomic groups analysed (including those determined by cytometry and optical microscopy) were classified in octave ($\log_2$) size classes. Abundance of each size class in logarithm scale was represented versus the $\log_{10}$ of the corresponding octave size. Similarities among SAS and physical, chemical and biological variables were analysed by principal component analysis in each

transect (PCA; Savenkoff et al. 1995, Packard et al. 2000). Two PCAs were performed. In the first case, the variables were SAS and micro-, nano- and picoplankton groups. In the second case, the variables were SAS and the hydrological variables (temperature, salinity, nutrients concentration and total chl *a*). Before performing the PCA, variables were transformed by subtracting the mean and dividing by the SD. The software STATISTICA 7.0 software (Stat. Soft., Inc.) was used for all the analysis.

RESULTS

Surface temperature in transect A increased from inshore towards offshore stations, varying between 15.65 and 17.58 ºC (Fig. 2A). Opposite to this, salinity exhibited lower values at the offshore stations, ranging from 37.03 at station 1 to 36.60 at station 5, with the minimum value being obtained at station 3 (36.38), which matches with a subminimum of temperature. This horizontal distribution of temperature and salinity suggests the presence of different water masses between coastal and open ocean stations and the presence of a geostrophic front located at station 3. Hydrological features in transect B were similar since the lowest temperature and highest salinity were obtained at station 1 (Fig. 2B). Besides, the horizontal distribution of hydrology suggests the presence of the geostrophic front at station 2.

In transect A, NO_3 and PO_4 concentrations showed similar variability patterns, increasing from station 1 towards station 3, where they reached the higher values at surface (thereafter SUP; 1.81 and 0.17 $\mu mol \cdot L^{-1}$, respectively) and at MSF depth (3.59 and 0.25 $\mu mol \cdot L^{-1}$, respectively; Fig. 3). Nutrient concentration decreased from station 3 to 5, reaching minimum values at station 5 (note that MSF depth increased towards open ocean). However, the variation range of NO_3 concentration was higher than that of PO_4. Moreover, in the case of NO_3, its concentration decreased below the detection limit at stations 4 and 5

at SUP depth, and at station 5 at MSF depth. The highest Chl *a* concentration was obtained at station 1 (1.69 $\mu g \cdot L^{-1}$). This maximum matched with low values of nutrient concentration. The low values of Chl *a* at stations 4 and 5 coincided with the lowest values of NO_3 concentration.

In transect B, NO_3 maximum concentration was obtained at station 1 (3.15 $\mu mol \cdot L^{-1}$ at SUP depth, and 3.38 $\mu mol \cdot L^{-1}$ at MSF depth; Fig. 3B), with a submaximun at station 3. Surface concentration at the other stations was below the detection limit. PO_4 decreased from inshore towards offshore stations, varying between 0.19 and 0.05 $\mu mol \cdot L^{-1}$ at surface and between 0.17 and 0.11 $\mu mol \cdot L^{-1}$ at MSF depth. Chlorophyll *a* concentration presented a peak in station 2 at both surface (2.23 $\mu g \cdot L^{-1}$) and MSF depths (2.62 $\mu g \cdot L^{-1}$), coinciding with low values of NO_3. Much lower concentrations of Chl *a* were obtained at the offshore stations (Fig. 3B).

Diatom abundance presented similar distributions in both transects and depths, with higher values at station 2, and minimum values at station 4, except in the transect A at MSF depth, where the minimum values were obtained at station 3 (Fig. 4). Flagellates abundance presented a similar variation pattern, with the highest value being found at station 2 in both transects (Fig. 4). In contrast, dinoflagellates abundance was homogeneous along transects and depths, except in transect B at MSF depth where it followed a pattern similar to diatoms and flagellates (Fig. 4).

The abundance of nano- and picoplankton was more variable than that of microplankton. *Prochlorococcus* abundance in transect A, increased from station 1 to 3, where it reached the maximum value ($12.96 \cdot 10^3$ cells$\cdot mL^{-1}$ at SUP depth, and $23.38 \cdot 10^3$ cells$\cdot mL^{-1}$ at MSF depth), and then decreased towards offshore stations (Fig. 5). In transect B, the pattern was similar at both depths, but with a lower range of variability (Fig. 5). *Synechococcus* in transect A decreased from station 1 to 3 with values very similar at surface and MSF

depths. Its abundance peaked at station 4 SUP but decreased at station 5 SUP to match the value at MSF depth. In transect B, *Synechococcus* abundance increased from station 1 towards station 5, with a lower variability than in transect A. Picoeukaryotes abundance peaked at stations 2 and 3 at SUP depth of transect A. However, at MSF depth, the variation pattern was different since a maximum value was obtained at station 1 ($28.60 \cdot 10^3$ cells·mL^{-1}). Nanoeukaryotes abundance in transect A showed a distribution similar to that obtained for diatoms and flagellates, with a maximum at station 2 ($6.48 \cdot 10^3$ cells·mL^{-1} at SUP depth, and $6.48 \cdot 10^3$ cells·mL^{-1}) and lower values at the offshore stations. However, in transect B, diatoms and flagellates decreased from inshore to offshore stations.

Diatoms was the dominant group of microplankton (>45%) in transect A, followed by flagellates and dinoflagellates, except in the surface sample of station 4 and in the MSF sample of station 5 where dinoflagellates was the dominant group (Table 2). Contrarily, in transect B, diatoms dominance decreased from station 1 towards station 5, while the percentage of flagellates increased until being the dominant group in the samples collected at station 4 SUP and station 5 MSF (Table 2). *Synechococcus* was the dominant group within the picoplankton in transect A, followed by picoeukaryotes, *Prochlorococcus* and nanoeukaryotes. Only in the sample collected at station 4 MSF, *Prochlorococcus* was the dominant group. In transect B, the relative abundance of *Synechococcus* increased from inshore towards offshore stations (from 33.38% to 91.92% at SUP depth, and from 29.90% to 79.02% at MSF depth). This group was dominant in all the samples except at station 1 where picoeukaryotes were dominant (Table 2).

Globally, SAS ranged from -0.70 to -0.88 in transect A and from -0.60 to -0.81 in transect B. There was not a homogeneous variation pattern of SAS with depth. The differences between surface and MSF depths were not statistically significant (Student t-test, $p>0.05$). Irrespective of these differences, SAS tended to decrease following the gradient coast-

offshore in both transects. In transect A, SAS at SUP depth increased from station 1 towards stations 2 and 3. The most negative value of SAS was obtained at station 5 (-0.87). At MSF depth, SAS and chl *a* showed a similar variability pattern, with a decreasing trend from station 1 towards station 3 and minimum values obtained at station 5 (-0.89) (Fig. 6). In transect B, the variability of SAS was similar at both depths and we found a significant correlation between SAS and chl a ($r^2 = 0.79$; $p < 0.05$). On average, SAS was more negative (-0.81 ± 0.07) in transect A than in B (-0.68 ± 0.09) indicating a higher predominance of lower size phytoplankton (Table 3).

In order to identify which phytoplankton groups contributed to the variability of SAS, a principal component analysis (PCA) was performed using the normalized abundance matrix. The two main factors obtained from PCA are shown in Figure 7A. Diatoms, flagellates and SAS contributed negatively to Factor 1 while *Synechococcus* did it positively. The correlation between SAS and Factor 2 was very low indicating that the variability in SAS was mainly due to variations in abundance of diatoms, flagellates and *Synechococcus*. The scores of the surface and MSF samples for Factor 1 indicate that the lowest SAS obtained in the coastal samples were due to a higher abundance of diatoms and flagellates. An additional PCA was performed to study the relationship between SAS and physical and biogeochemical variables. The two main factors obtained are shown in Figure 7B. Nutrient concentration, salinity, chl *a* and SAS contributed positively to Factor 1, while temperature did it negatively. It is notably that very low nutrient concentrations were related with the low concentration of chl *a* and major relevance of picophytoplankton. Consequently, this factor could be considered representative of the hydrological gradient existing from coast to open ocean. On the other hand, Factor 2 did not show differences between transects or depths.

DISCUSSION

The Atlantic jet that penetrates through the Strait of Gibraltar feeds different permanent hydrological structures that determine the spatial distribution of nutrients and chlorophyll *a* in the Alborán basin (Cortés et al., 1985; Minas et al., 1991; Rodríguez et al., 1997). Different upwelling zones are distributed along the coastline in association with the geostrophic front produced by the Atlantic jet, where the deeper Mediterranean water, enriched in inorganic nutrients, reaches the surface layer (Minas et al., 1991; LaFuente et al., 1998; Rodríguez et al., 1998; Sharhan et al. 2000). One of these upwelling areas is located off the coast of Málaga, where the water column is normally characterised by the presence of two layers. The upper layer corresponds to Atlantic water more or less modified (AW) that features 36.5 salinity and very low nutrient concentrations. The deeper layer is colder and saltier Mediterranean water (MW) with relatively high nutrient concentrations. The thickness of the AW layer is quite variable depending on the velocity and position of the Atlantic jet, the seasonal cycle period (normally, it is much reduced in spring) and the wind regime (Ramírez et al., 2005; Mercado et al. 2005). Also, westerlies blowing along the coast of Málaga favour the upwelling of the MW resulting in enrichment of the surface layer. This wind regime is more frequent in spring, coinciding with a lower thickness of the AW layer (Mercado et al., 2007). During the two-three days before our samplings, westerlies were predominant in the study area (data not shown). These winds would have favoured the upwelling, which explains the relatively high surface salinity obtained in the coastal stations, as well the conspicuous gradient of temperature and salinity located between stations 2 and 3 in both transects. At the offshore stations of both transects, the values of surface salinity were similar to those expected for unmodified AW, indicating that these stations were probably located within the western

anticyclonic gyre. This hydrological pattern could be considered characteristic of the springtime.

Nutrient concentrations followed a variation pattern similar to salinity. Thus, the lower concentrations of nitrate and phosphate were obtained at the surface of offshore stations (4 and 5). In contrast, the higher concentrations of nutrients were found in the stations located on the geostrophic front. In fact, salinity, nitrate and phosphate concentrations were strongly correlated. It is expected that chlorophyll a followed a pattern similar to nutrients. Accordingly, very low chlorophyll a concentration was observed at the offshore stations. However, high concentrations of chl a were associated with relatively low nitrate concentrations in transect B (station 2); whereas the highest concentrations of nitrate in the transect A were obtained in station 3, where the chl a concentrations were relatively low. These results indicate that the phytoplanktonic communities sampled in each transect were at different phases of the bloom induced by the upwelling. The upwelling brings water enriched in nutrients to the surface layer, promoting the growth of the phytoplankton. According to the early observation by Margalef (1978), the succession pattern following an upwelling event is characterized by a rapid growth of diatoms well-adapted to high turbulence and nutrient repletion conditions, situation that we found at station 3 of transect A. In the next step of the succession, the phytoplanktonic community would reach an abundance peak, after which the cells would sink out the euphotic zone and be replaced by a community composed of larger diatoms, flagellates and dinoflagellates (Estrada and Blasco, 1985; Fernandes and Brandini, 2004; Lassiter et al, 2006; among others). This was the case of station 2 in transect B, where the low nitrate concentration matched the maximum chl a concentration.

Irrespective of the hydrological differences, the chlorophyll *a* concentration variability was associated with changes in abundance of diatoms ($r^2 = 0.52$; Student t-test $p < 0.05$), which

were less abundant at offshore stations. The horizontal distribution of the phytoplankton along the gradient coast-open ocean observed in our study could be considered concordant with the paradigm of dominance of large cells in productive areas, in contrast to oligotrophic open ocean areas where small cells dominante (Steele, 1974; Azam et al., 1983). However, relatively high values of chl *a* were obtained at station 1 of transect A where the diatom abundance was low. This high values of chl *a* may be due to a high concentration of chl *a* per cell in diatoms or to a major contribution of picoeukaryotes and nanoeukaryotes to the total chl *a*, which showed a distribution pattern similar to diatoms, being this size fraction associated with the upwelling.

From a physiological point of view, small cells require lower nutrient concentrations in the surrounding medium than larger cells to keep an equivalent influx per volume unit (Armbrust and Chisholm, 1992). Thus, being the availability of nutrients higher at MSF depth, the microplankton abundance would be higher. However, although the nutrient concentration found in our survey was major at MSF than at surface, the microplankton abundance was only higher at MSF at coastal stations (1 and 2), except diatoms in transect B and flagellates in transect A, with similar values along the other stations. Therefore, at coastal stations, like the relative abundance of microplankton was higher than nano- and picoplakton, the SAS at MSF depth was less negative than at surface. Along the two transects sampled, SAS decreased from inshore to offshore stations, following the predicted behaviour: a decrease in chlorophyll concentration linked with the decrease in diatoms abundance towards open ocean resulting in more negative values of SAS (Harris et al., 1987; Chisholm, 1992). However, there were stations where SAS at MSF was more negative than at surface. In transect A, SAS presented lower values than in transect B, because diatoms abundance in transect A was lower than in transect B, while *Synechococcus* abundance was higher in transect A. In transect A, SAS value at surface

was similar at stations 1 and 5, where SAS is minimum. This was probably due to the low diatoms and flagellates abundance in relation with the high abundance of picoeukaryotes and nanoeukaryotes.

The differences in phytoplanktonic composition of inshore stations observed between transects suggests that the diatom communities in each transect represented different bloom phases (Fig. 8). Mercado et al. (in press) described four diatom communities at coastal upwelling areas. Two of them, characteristic of the surface layer, are concordant with the communities found in our survey. Despite the salinity being similar in both transects, the community dominated by *Chaetoceros sp.*, correspondent to the station 1 of transect B, was associated with water masses colder than community the dominated by *Leptocylindrus sp.*, correspondent to the station 1 of transect A. These differences in temperature could be attributed to differences in the residence time of the upwelled waters in the surface layer. In other words, the community dominated by *Chaetoceros sp.* is associated to colder waters representing the first phase of the bloom, when the nutrient concentration in the recently upwelled waters is relatively high (in special nitrate). In contrast, the community dominated by *Leptocylindrus sp*. would dominate when the upwelling relaxes and the nutrients begin to decline, being the community dominated by *Chaetoceros* replaced by the one dominated by *Leptocylindrus*. Along our transect A, the predominant community associated was the type (2) with *Leptocylindrus sp*. as dominant specie (Fig. 8). We found the same situation at offshore surface stations of transect B. However, at inshore stations of transect B and at station 2 in transect A, *Chaetoceros sp*., characteristic of the first phase of the bloom, was the dominant species (Fig. 8).

It is notably that these differences in composition of microplankton, which are indicative of different hydrological situations and probably result in physiological and functional differences. However, in our study a clear relationship between SAS and species

composition of diatoms was not obtained. For instance, phytoplankton assemblages dominated by *Leptocylindrus sp*. featured different SAS values. Consequently, the utility of SAS as an adequate indicator of physiological properties of the phytoplankton assemblages should be revised. Irrespective of this, our data support the hypothesis that communities with values of SAS less negatives are characteristics of waters rich in nutrients, while oligotrophic waters where the relative importance of picoplankton is higher are characterized by lower SAS values.

ACKNOWLEDGMENTS

This work is a contribution to project TROFOALBORAN (CTM2009-07776/MAR) of the Spanish National Programme in Marine Science and Technology from the Ministerio Español de Innovacion y Ciencia (co-funded by EU). Iria Sala was supported by a studentship of the Ministerio de Educación.

REFERENCES

Armbrust, E.V., Chisholm, S.V., 1992. Patterns of cell-size change in a marine centric diatom. Variability evolving from clonal isolates. Journal of Phycology, 28:146-156.

Azam F., Fenchel T., Field J.G., Gray J.S., Meyer-Reil L.A. and Thingstad F., 1983. The ecological role of water-column microbes in the sea. Marine Ecology Progress Series 10, 257–263.

Chisholm SW, 1992. Phytoplankton size. In: Falkowski PG, Woodhead AD (eds) Primary productivity and biogeochemical cycles in the sea. Plenum Press, New York, p 213–217

Cortés, D., Gil, J. and García, A, 1985. General distribution of chlorophyll, temperature and salinity in the north-western sector of Alboran Sea. Communication from the XXIX Congres-Assemblee pleniere CIESM. Lucerne, 11-19.

Delgado, M., 1990. Phytoplankton distribution along the Spanish coast of the Alboran Sea. Scientia Marina, 54 :169-178

Estrada, M. and Blasco., D., 1985. Phytoplankton assemblages in coastal upwelling areas. In: International Symposium on the most important Upwelli Areas off Western Africa (Cape Blanco and Benguela). C. Bas, R. Margalef and P. Rubíes (eds.) 1: 379-402. Instituto de Investigaciones. Pesqueras. Barcelona.

Fernandes, L.F., and Brandini, F.P., 2004. Diatom associations in shelf waters of Paraná state, Southern Brazil: annual variation in relation to environmental factors. Bazilian Journal of Oceanography, 52: 19-34.

Harris, G. P., Ganf, G. G. and Thomas, D. P., 1987. Productivity, growth rates and cell size distributions of phytoplankton in the SW Tasman Sea: implications for carbon metabolism in the photic zone. J. Plankton Res. 9, 1003-1030.

Lafuente, J.G., Cano, N., Vargas, M., Rubín, J.P., Hernández-Guerra, A., 1998. Evolution of the Alboran Sea hydrographic structures during July 1993. Deep-Sea Research I 45,

39–65.

Lassiter, A.M., Wilkerson, F.P., Dugdale R.C., and Hogue, V.E., 2006. Phytoplankton assemblages in the CoOP_WEST coastal upwelling area. Seep-Sea Research II 53:3063-3077.

Legendre, L., Le Fèvre, J., 1991. From individual plankton cells to pelagic marine ecosystems and to global biogeochemical cycles. In: Demers S (ed) Particle analysis in oceanography. Springer-Verlag, Heidelberg, p 261–300.

Margalef, R., 1978. Life forms of phytoplankton as survival alternatives in an unstable environment. Oceanologica Acta 1, 493–509.

Mercado, J.M., Ramírez, T., Cortés, D., Sebastián, M., Vargas, M., 2005. Temporal changes of the phytoplankton communities in an upwelling area of the Alborán Sea. Scientia Marina 69 (4), 451–465.

Mercado, J.M., Cortés, D., García, A., & Ramírez, T., 2007. Seasonal and Inter-annual changes in the planktonic communities of the northwest Alboran Sea (Mediterranean Sea). Progress in Oceanography, 74:273-293.

Mercado, J.M., Ramírez, T., Cortés, D., Sebastián, M., Reul, A., & Bautista, B., 2006. Diurnal changes in the bio-optical properties of the phytoplankton in the Alborán Sea (Mediterranean Sea). Estuarine Coastal and Shelf Science, 69, 459-470.

Minas, H.J., Coste, B., LeCorre, P., Minas, M. and Raimbault, P., 1991. Biological and geochemical signatures associated with the water circulation through the Strait of Gibraltar and in western Alboran Sea. *J. Geophys. Res.*, 96: 8755-8771.

Olenina, I., Hajdu, S., Edler, L., Andersson, A., Wasmund, N., Busch, S., Göbel, J., Gromisz, S., Huseby, S., Huttunen, M., Jaanus, A., Kokkonen, P., Ledaine, I. and Niemkiewicz, E., 2006. Biovolumes and size-classes of phytoplankton in the Baltic Sea. HELCOM Balt.Sea Environ. Proc. No. 106, 144 pp.

Packard, T., Chen, W., Blasco, D., Savenkoff, C. and others, 2000. Dissolved organic carbon in the Gulf of St. Lawrence. Deep-Sea Res II 47:435–459

Parrilla,. G. and Kinder, T. H., 1985. The physical oceanography of the Alborán Sea. NATO Advanced Research Workshop. LQ Specia, 7-14 September 1983. Proceedings. Charnock, H. (ed) pp. 1-23.

Parrilla, G. and Kinder, T. H., 1987. Oceanografía física del Mar de Alborán. Bol. Inst. Esp. Oceanogr., 4(1): 133-165.

Raimbault, P., Rodier, M., Taupier-Letage, I., 1988. Size fraction of phytoplankton in the Ligurian Sea and the Algerian Basin (Mediterranean Sea): size distribution versus total concentration. Mar Microb Food-Webs 3:1–7

Ramírez, T., Cortés, D., Mercado, J.M., Vargas-Yañez, M., Sebastián, M., Liger, E., 2005. Seasonal dynamics of inorganic nutrients and phytoplankton biomass in the NW Alboran Sea. Estuarine Coastal and Shelf Science 65, 654–670.

Ribes, M., Coma, R. and Gili J. M., 1999. Seasonal variation of particulate organic carbon, dissolved organic carbon and the contribution of microbial communities to the live particulate organic carbon in a shallow near-bottom ecosystem in the Northwestern Mediterranean Sea. J. Plankton Res., 21, 1077-1100.

Rodríguez, V., Blanco, J. M., Jiménez-Gómez, F., Rodríguez, J., Echevarría, F. and Guerrero, F., 1997. Distribución espacial de algunos estimadores de biomasa fitoplanctónica y material orgánico particulado en el mar de Alborán, en condiciones de estratificación térmica (julio de 1993). Publ. Espec. Inst. Esp. Oceanogr., 24: 53-64.

Rodríguez, J., Blanco, J. M., Jiménez-Gómez, F., Echevarría, F., Gil, J., Rodríguez, V., Ruiz, J., Bautista, B., Guerrero, F., 1998. Patterns in the size structure of the phytoplankton community in the deep fluorescence maximum of the Alboran Sea (southwestern Mediterranean). Deep-Sea Res 45:1577–1593

Savenkoff, C., Chanut, J. P., Vezina, A. F., Gratton, Y., 1995. Distribution of biological-activity in the lower St. Lawrence estuary as determined by multivariate analysis. Estuar Coast Shelf Sci 40:647–664

Sharhan, T., García-LaLafuente, J., Vargas, M., Vargas, J.M., Plaza, P., 2000. Upwelling mechanisms in the northwestern Alborán Sea. Journal of Marine System 23, 317–331.

Steel, J. H. (1974) The structure of marine ecosystems. Harvard University Press, Cambridge.

Sun, J. and Liu, D., 2003. Geometric models for calculating cell biovolume and surface area for phytoplankton. J. Plankton Res., 25: 1331-1346.

Thingstad, T. and Sakshaug E., 1990. Control of phytoplankton growth in nutrient recycling ecosystems. Theory and terminology. Mar. Ecol. Porg. Ser., 63, 261-272.

Tintoré, J., Gomis, D., Alonso, S., Parrilla, G., 1991. Mesoscale Dynamics and Vertical Motion in the Albora´n Sea. Journal of Physical Oceanography 21 (6), 811–823.

Tomas, C.R., 1997. Identifying Marine Phytoplankton. Academic Press Limited, London.

Utermöhl, H., 1958. Zur Vervollkommnung der quantitativen Phytoplankton-Methodik. Mitt. int Verein. Limnol., 9: 1-38.

Vadrucci, M. R., Cabrini, M. and Basset, A., 2007. Biovolume determination of phytoplankton guilds in transitional water ecosystems of Mediterranean Ecoregion. TWB, Transit. Waters Bull. 2(2007), 83-102.

Vaulot, D., Courties, C., Partensky, F., 1989. A simple method to preserve oceanic phytoplankton for flow cytometric ananlysis. Cytometry 10, 629–635.

FIGURE LEGENDS

Figure 1. Sampling area: NW Alborán Sea.

Figure 2. Temperature (ºC) and salinity variations along transects A and B at surface depth (5 m).

Figure 3. NO_3 ($\mu mol \cdot L^{-1}$), PO_4 ($\mu mol \cdot L^{-1}$) and Chl *a* ($\mu g \cdot L^{-1}$) concentrations along transects A and B at surface (open circles) and maximum subsurface fluorescence (MSF, filled circles) depths. The numbers near the filled circles indicate the depth in meters of MSF at each station.

Figure 4. Abundance distribution of diatoms, dinoflagellates and flagellates ($cells \cdot mL^{-1}$) along transects A and B at surface (open circles) and MSF (filled circles) depths.

Figure 5. Abundance distribution of *Prochlorococcus*, *Synechococcus*, picoeukaryotes and nanoeukaryotes (10^3 $cells \cdot mL^{-1}$) along transects A and B at surface (open circles) and MSF (filled circles) depths.

Figure 6. Size-abundance spectra (SAS) variations along transects A and B at surface (open circles) and MSF (filled circles) depths.

Figure 7. Principal component analysis showing the relationship between SAS and the phytoplankton groups abundance (A); and between SAS and physical and biogeochemical variables (B).

Figure 8. Community diatoms composition at each station and depth along transects A and B.

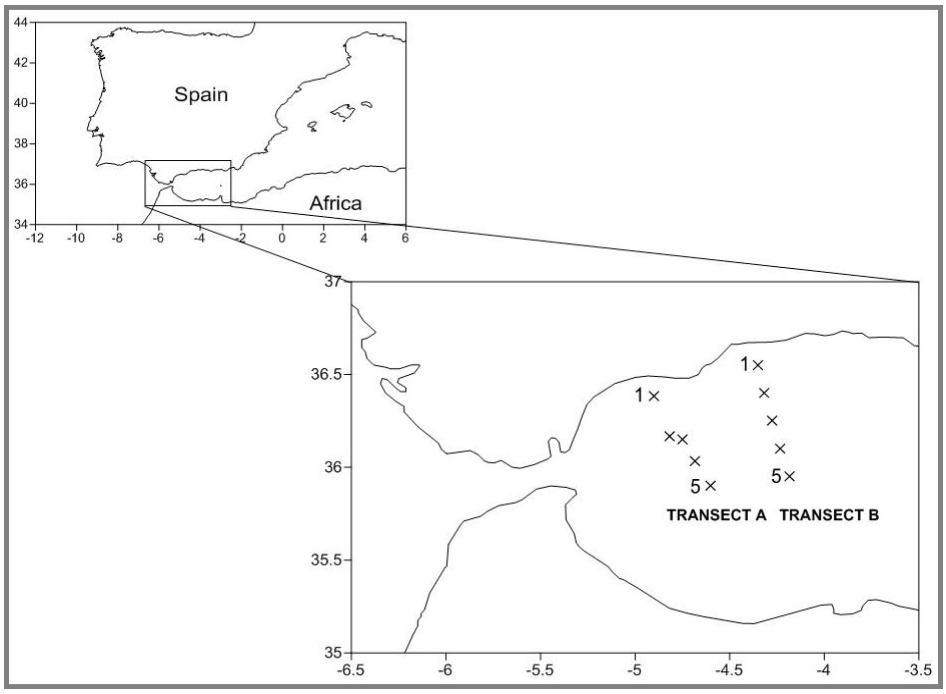

Figure 1.

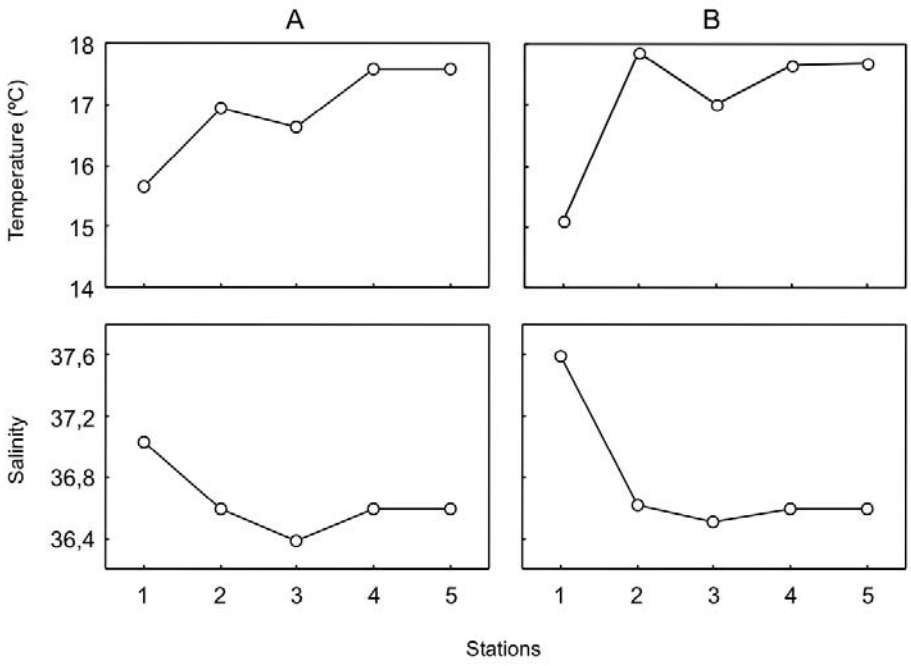
A
B
Temperature (°C)
18
17
16
15
14
Salinity
37,6
37,2
36,8
36,4
1
2
3
4
5
Stations

Figure 2.

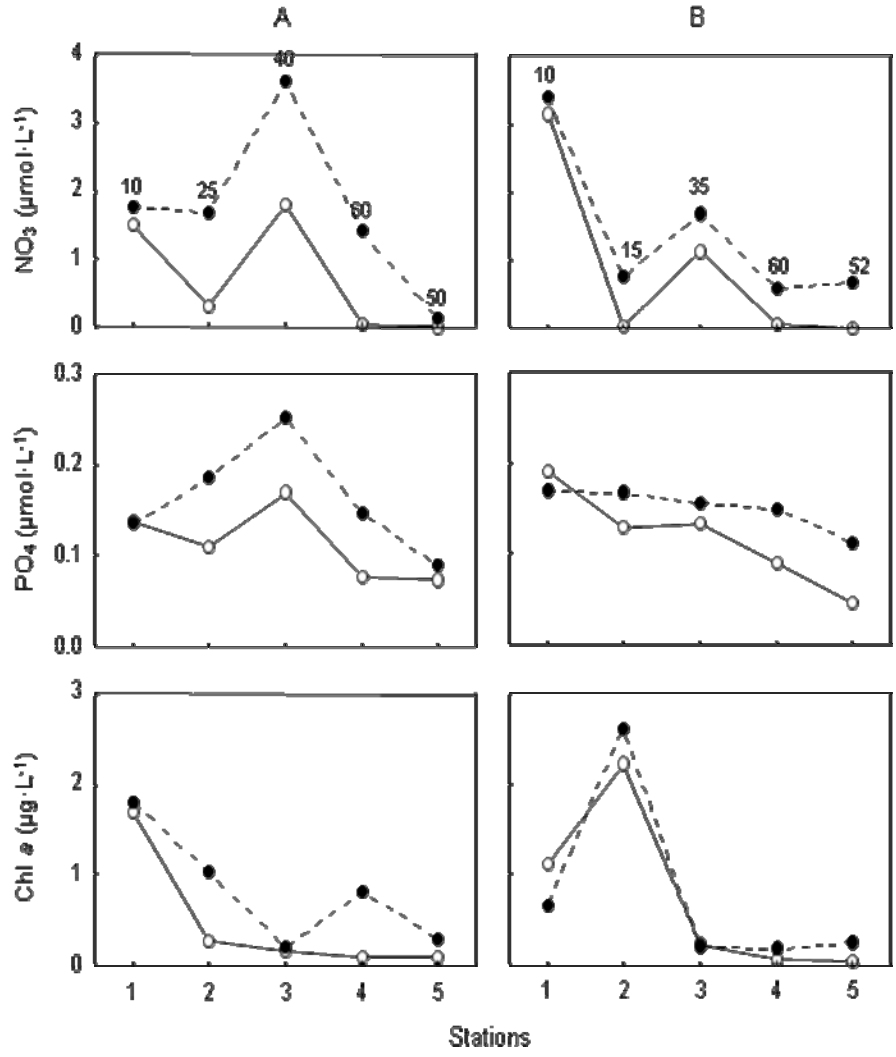
A
B
NO_3 (µmol·L^{-1})
PO_4 (µmol·L^{-1})
Chl *a* (µg·L^{-1})
10
25
40
60
50
10
15
35
60
52
Stations

Figure 3.

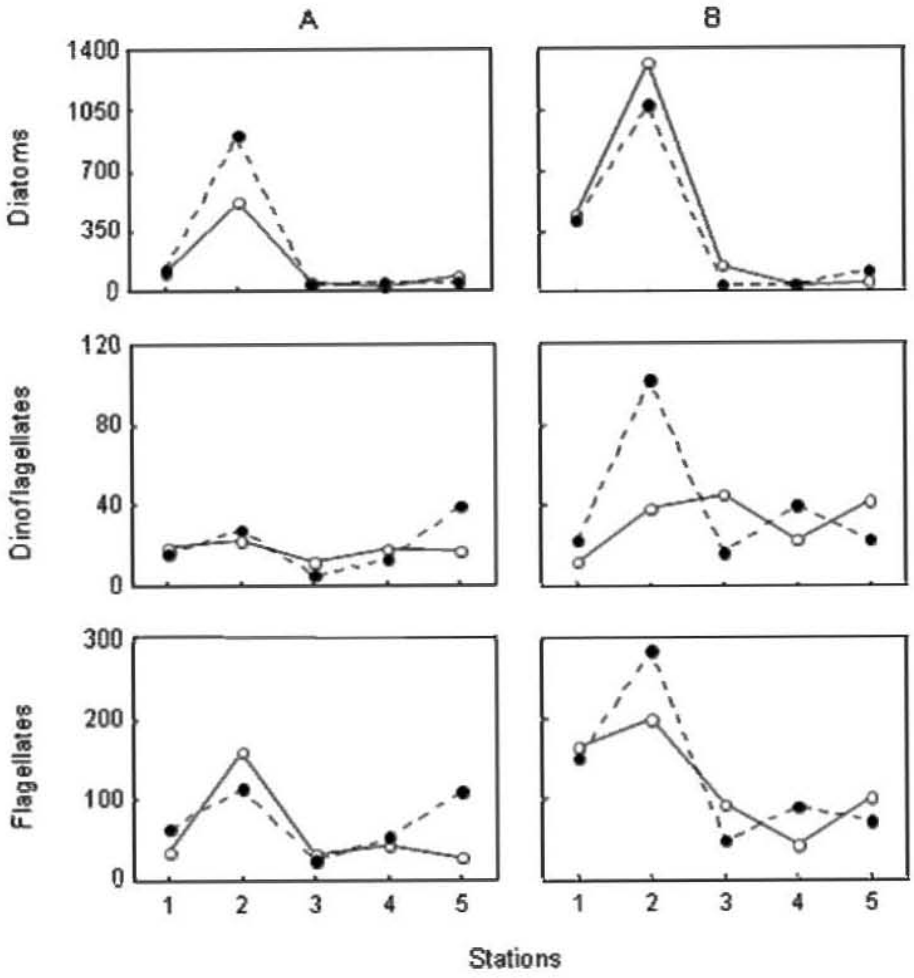
A
B
Diatoms
1400
1050
700
350
0
Dinoflagellates
120
80
40
0
Flagellates
300
200
100
0
1
2
3
4
5
Stations

Figure 4.

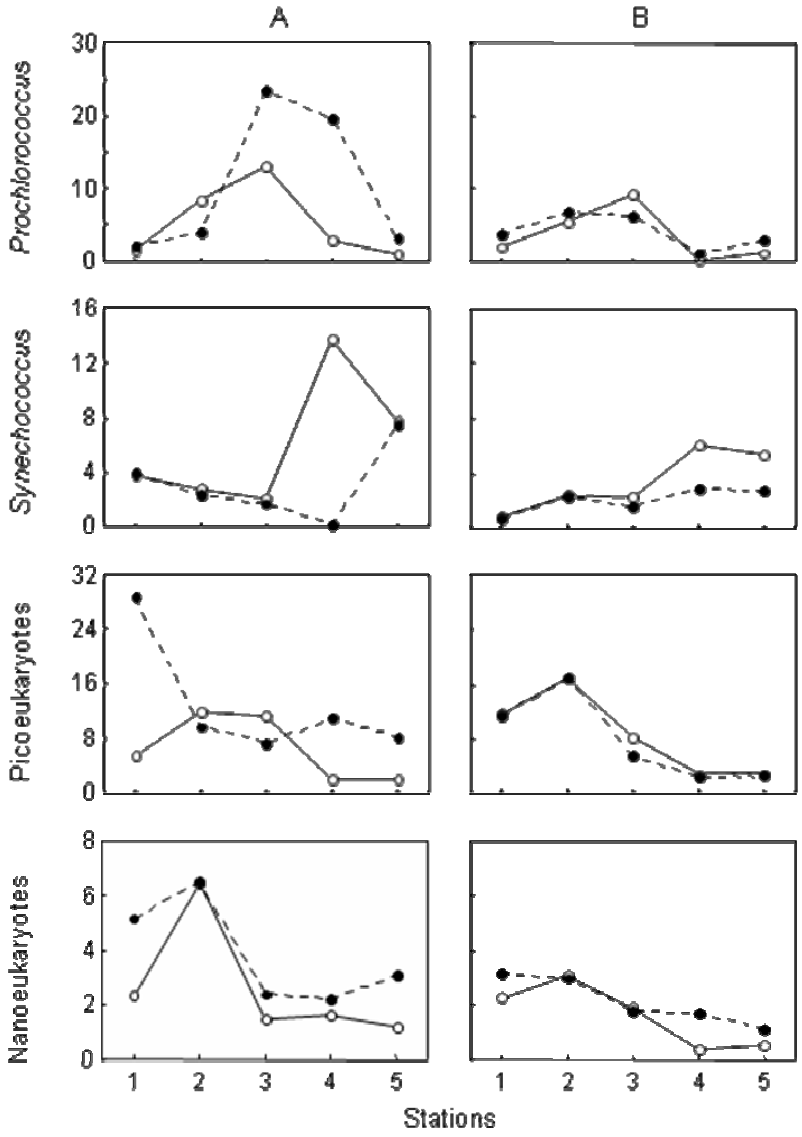
A
B
Prochlorococcus
Synechococcus
Picoeukaryotes
Nanoeukaryotes
30
20
10
0
16
12
8
4
0
32
24
16
8
0
8
6
4
2
0
1
2
3
4
5
Stations

Figure 5.

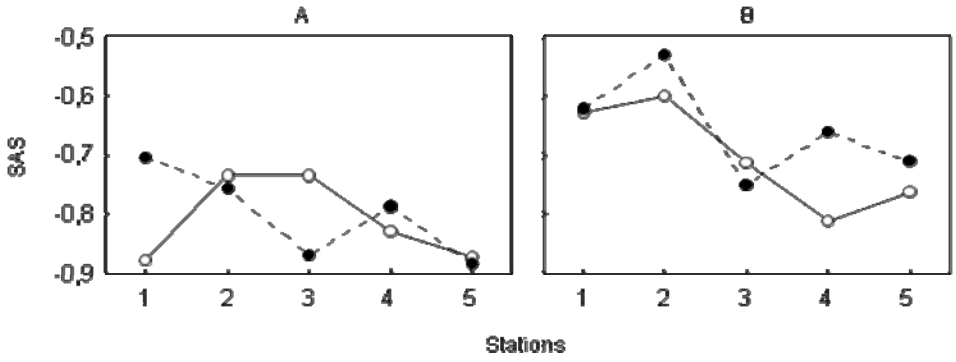

Figure 6.

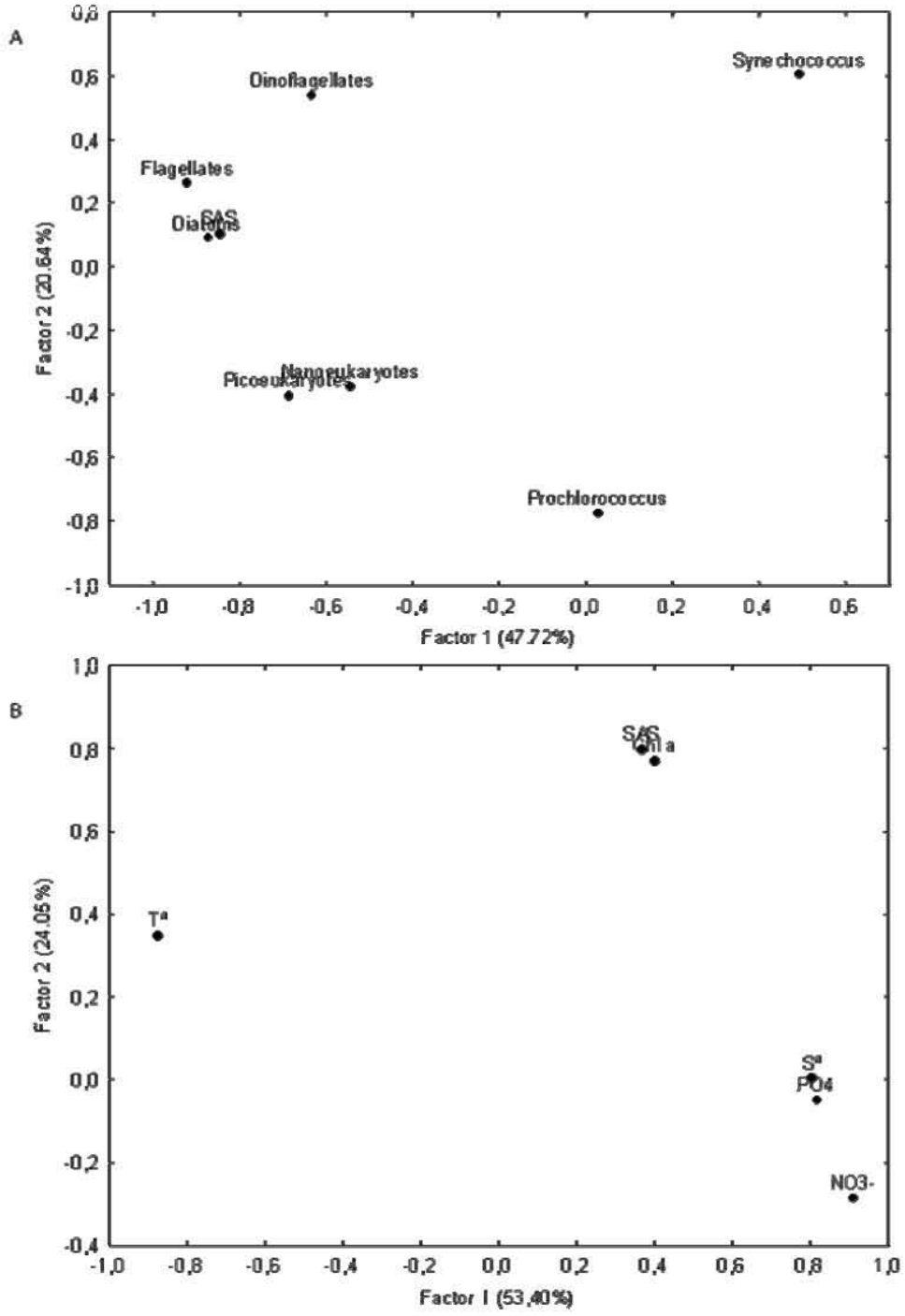
A
Synechococcus
Dinoflagellates
Flagellates
SAS
Diatoms
Nanoeukaryotes
Picoeukaryotes
Prochlorococcus
Factor 2 (20.64%)
Factor 1 (47.72%)
B
SAS
Chla
T°
Si
PO4
NO3-
Factor 2 (24.05%)
Factor I (53,40%)

Figure 7.

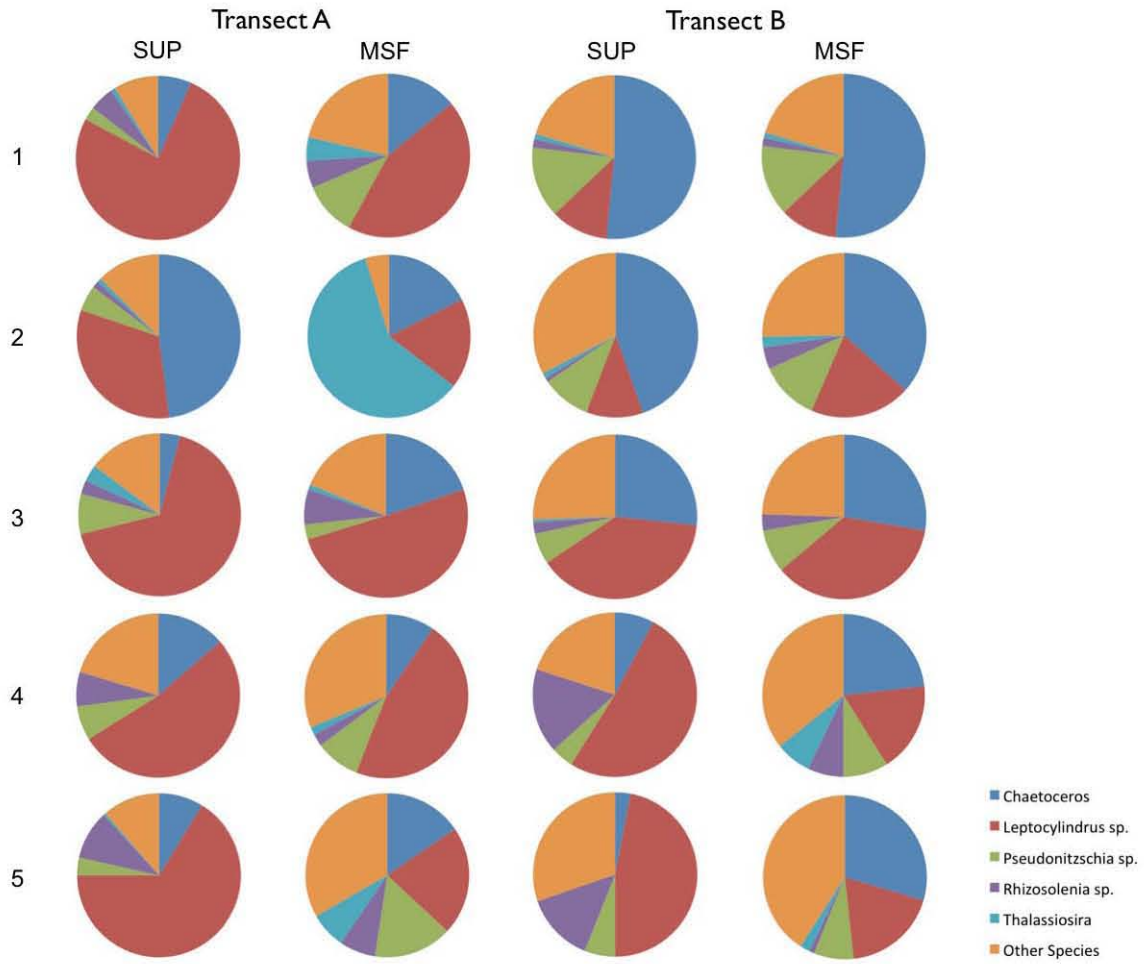
Transect A
Transect B
SUP
MSF
SUP
MSF
1
2
3
4
5
Chaetoceros
Leptocylindrus sp.
Pseudonitzschia sp.
Rhizosolenia sp.
Thalassiosira
Other Species

Figure 8.

Table 1. Geometric formulas applied to calculate cell biovolume from length measurements of the different species of phytoplankton identified and mean species biovolume (±SD) obtained. N: number of measured cells of each specie; V: cell biovolume; d: cell diameter; h and b: cell height; c: cell width, which in diatoms is assumed to be equal to b, except in *Pseudonitzschia* where c = (b -1); in dinoflagellates c is assumed to be a 67% of b, except in *Ceratium spp*. where c = b, and *Prorocemtrum spp*. Where c is a 55% of b.

Taxonomic Group	Species	Formula	Reference	Biovolume (µm3)	N
Diatoms	*Asterionellopsis glacialis*	$V = \frac{\pi}{12} d^2 h$ - 40%	Olenina et al., 2006	45.51 ± 12.70	129
	Bacteriastrum spp.	$V = \frac{\pi}{4} d^2 h$	Vraducci et al. 2007	8507.01 ± 9266.83	19
	Cerataulina spp.	$V = \frac{\pi}{4} d^2 h$	Vraducci et al. 2007	18492.54 ± 3345.49	14
	Chaetoceros spp.	$V = \frac{\pi}{4} d^2 h$	Vraducci et al. 2007	3453.44 ± 3345.49	86
	Cylindrotheca spp.	$V = \left(\frac{\pi}{6} d^2 h\right) + \left(\frac{\pi}{2} d_m^2 h_m\right)$	Vraducci et al. 2007	2629.53 ± 140.91	13
	Eucampia spp.	$V = \frac{\pi}{4} a b c$	Vraducci et al. 2007	20232.74 ± 10937.37	17
	Fragilariopsis spp.	$V = \frac{\pi}{4} a b c$	Vraducci et al. 2007	1363.46 ± 1081.59	4
	Guinardia spp.	$V = \frac{\pi}{4} d^2 h$	Vraducci et al. 2007	48455.61 ± 67172.55	6
	Guinardia delicatula	$V = \frac{\pi}{4} d^2 h$	Vraducci et al. 2007	8155.61 ± 7692.27	27
	Guinardia flacida	$V = \frac{\pi}{4} d^2 h$	Vraducci et al. 2007	127190.37 ± 118386.9	6
	Guinardia striata	$V = \frac{\pi}{4} d^2 h$	Vraducci et al. 2007	40146.37 ± 22088.59	7

	Leptocylindrus spp.	$V=\frac{\pi}{4}d^2h$	Vraducci et al. 2007	2401.72 ± 1298.75	70
	Leptocylindrus mediterraneus	$V=\frac{\pi}{4}d^2h$	Vraducci et al. 2007	25511.43 ± 52671.56	29
	Leptocylindrus minimus	$V=\frac{\pi}{4}d^2h$	Vraducci et al. 2007	758.08 ± 498.51	65
	Lioloma spp.	$V=\frac{\pi}{4}d^2h$	Vraducci et al. 2007	2411.49 ± 1468.81	3
	Meuniera spp.	$V=\frac{\pi}{4}abc$	Sun and Liu, 2003	28766.99 ± 16395.60	8
	Navicula spp.	$V=\frac{\pi}{4}abc$	Vraducci et al. 2007	2361.67 ± 2958.13	11
	Nitzschia spp.	$V=\frac{1}{2}abc$	Vraducci et al. 2007	642.82 ± 428.00	22
	Nitzschia longissima	$V=\frac{\pi}{4}d^2h$	Olenina et al., 2006	1000.88 ± 485.63	16
	Pleurosigma spp.	$V=\frac{1}{2}abc$	Vraducci et al. 2007	86306.78	1
	Pseudonitzschia spp.	$V=\frac{1}{2}abc$	Vraducci et al. 2007	1309.56 ± 1210.65	117
	Rhizosolenia spp.	$V=\frac{\pi}{4}d^2h$	Vraducci et al. 2007	90752.54 ± 191083.00	19
	Skeletonema spp.	$V=\frac{\pi}{4}d^2h$	Vraducci et al. 2007	1401.61 ± 781.27	17
	Thalassiosira spp.	$V=\frac{\pi}{4}d^2h$	Vraducci et al. 2007	13302.36 ± 10281.84	24
Dinoflagellates	*Ceratium spp.*	$V=\left(\frac{\pi}{6}ach\right)+\left(\frac{\pi}{6}d_m z_m\right)+\left(\frac{\pi}{4}d_1^2 h_1\right)$	Vraducci et al. 2007	137635.72 ± 135671.22	7
	Ceratium fusus	$V=\frac{\pi}{4}d^2h$	Vraducci et al. 2007	45839.60 ± 8764.36	3
	Dinophysis spp.	$V=\frac{\pi}{6}acb$	Olenina et al., 2006	10830.15 ± 5932.64	2
	Diplopsalis spp.	$V=\frac{\pi}{6}d^3$	Olenina et al., 2006	943.78	1
	Gymnodinium spp.	$V=\frac{\pi}{6}acb$	Olenina et al., 2006	8897.94 ± 30623.63	17

	Gyrodinium spp.	$V=\frac{\pi}{6}a\,c\,h$	Olenina et al., 2006	10937.77 ± 24568.99	26
	Oxitoxum spp.	$V=\frac{\pi}{4}d^2h$	Vraducci et al. 2007	1625.07	1
	Peridinium spp.	$V=\frac{\pi}{4}d^2h$	Vraducci et al. 2007	9960.46 ± 6831.25	8
	Prorocentrum spp.	$V=\frac{\pi}{6}a\,c\,h$	Olenina et al., 2006	166.71 ± 48.62	3
	Protoperidinium spp.	$V=\frac{\pi}{6}d^2h$	Vraducci et al. 2007	45576.63 ± 404847.09	9
	Scrippsiella	$V=\frac{\pi}{12}d^2h$	Olenina et al., 2006	1203.87 ± 1064.86	7
	Ellipsoid Dinoflagellate	$V=\frac{\pi}{6}d^2h$	Vraducci et al. 2007	21499.94 ± 52362.40	14
	Sphere Dinoflagellate	$V=\frac{\pi}{6}d^3$	Vraducci et al. 2007	5012.35 ± 9753.48	41
Flagellates	*Dictyocha spp.*	$V=\frac{\pi}{12}d^3$	Olenina et al., 2006	13927.68	1
	Euglena spp.	$V=\frac{\pi}{6}d^2h$	Olenina et al., 2006	369.81 ± 143.90	3
	Ellipsoid Flagellate	$V=\frac{\pi}{6}d^2h$	Vraducci et al. 2007	251.03 ± 233.23	19
	Sphere Flagellate	$V=\frac{\pi}{6}d^3$	Vraducci et al. 2007	304.92 ± 339.54	127

Table 2. Relative abundances of microplankton and nano- and picoplankton groups along transects A and B.

		Microplankton abundance (%)			Nano- and Picoplankton abundance (%)			
Transect	Station	Diatoms	Dinoflagellates	Flagellates	Prochlorococcus	Synechococcus	Picoeukaryotes	Nanoeukaryotes
A SUP	1	67.16	11.54	21.30	3.55	80.39	11.16	4.90
	2	74.42	3.16	22.42	15.26	51.53	21.59	11.62
	3	52.84	12.06	35.11	27.90	44.61	24.32	3.17
	4	25.00	22.46	54.24	2.02	95.49	1.38	1.11
	5	67.66	13.06	19.29	1.17	94.81	2.51	1.51
A MSF	1	61.10	7.54	31.36	2.81	52.47	37.84	6.88
	2	86.36	2.67	10.97	8.69	55.24	21.48	14.59
	3	53.44	9.52	37.04	46.44	34.47	14.26	4.84
	4	45.13	10.47	44.40	55.96	5.91	31.81	6.32
	5	22.95	20.49	56.56	3.67	84.00	8.82	3.50
B SUP	1	71.45	1.96	26.60	8.88	33.28	48.41	9.43
	2	84.90	2.47	12.64	10.95	48.85	34.00	6.20
	3	51.58	15.76	32.66	22.36	53.45	19.68	4.52
	4	36.73	22.04	41.22	0.55	94.18	4.58	0.69
	5	26.40	21.60	52.00	2.41	91.92	4.72	0.94
B MSF	1	69.99	3.90	26.12	14.93	29.20	43.53	12.33
	2	73.78	6.95	19.27	14.06	45.21	34.63	6.09
	3	38.06	15.79	46.15	21.49	52.76	19.76	5.99
	4	20.14	24.10	55.76	3.79	84.82	6.35	5.04
	5	55.92	10.47	33.61	9.66	79.02	7.91	3.41

Table 3. Regression coefficients of the size-abundance spectra (SAS) model log along transects A and B at surface (SUP) and MSF depths. (*: p<0.05, **: p<0.01, ***p<0.001).

Transect	Station	a	SAS (b)	R^2
A SUP	1	4.087	-0.877	0.76***
	2	4.047	-0.736	0.72***
	3	3.389	-0.736	0.59**
	4	3.397	-0.830	0.48*
	5	3.948	-0.873	0.63**
A MSF	1	3.669	-0.703	0.59**
	2	3.983	-0.757	0.54**
	3	3.566	-0.869	0.65**
	4	3.610	-0.786	0.72***
	5	4.248	-0.885	0.79***
B SUP	1	3.704	-0.627	0.73***
	2	3.974	-0.601	0.71***
	3	3.622	-0.714	0.62**
	4	3.743	-0.810	0,66**
	5	3.794	-0.761	0.67**
B MSF	1	3.706	-0.622	0.69**
	2	3.850	-0.529	0.64**
	3	3.413	-0.750	0.65**
	4	3.184	-0.661	0.47*
	5	3.576	-0.712	0.71***